



Published in final edited form as:

*NMR Biomed.* 2008 February ; 21(2): 159–164. doi:10.1002/nbm.1173.

## Intracellular Water Specific MR of Microbead-adherent Cells: The HeLa Cell Intracellular Water Exchange Lifetime

L. Zhao, C. D. Kroenke, J. Song, D. Piwnica-Worms, J. J. H. Ackerman, and J. J. Neil

From Departments of Chemistry (L.Z., J.J.H.A.), Internal Medicine (J.J.H.A.), Molecular Biology and Pharmacology (D.P.-W.), Neurology (J.J.N.), Pediatrics (J.J.N.) and Radiology (C.D.K., J.S., D.P.-W., J.J.H.A., J.J.N.), Washington University, One Brookings Drive, St. Louis, Missouri 63130.

### Abstract

Quantitative characterization of the intracellular water  $^1\text{H}$  magnetic resonance (MR) signal from cultured cells will provide critical biophysical insight into the MR signal from tissues *in vivo*. Microbeads provide a robust immobilization substrate for the many mammalian cell lines that adhere to surfaces and also provide sufficient cell density for observation of the intracellular water MR signal. However, selective observation of the intracellular water MR signal from perfused, microbead-adherent mammalian cells requires highly effective suppression of the extracellular water MR signal. We describe herein how high velocity perfusion of microbead-adherent cells results in short *apparent*  $^1\text{H}$  MR longitudinal and transverse relaxation times for the extracellular water in a thin slice selected orthogonal to the direction of flow. When combined with a spin echo pulse sequence, this phenomenon provides highly effective suppression of the extracellular water MR signal. This new method is exploited herein to quantify the kinetics of water exchange from the intracellular to extracellular spaces for HeLa cells. The time constant describing water exchange from intracellular to extracellular spaces, also known as the exchange lifetime for intracellular water, is  $119 \pm 14$  ms.

### Keywords

intracellular water selection; extracellular water suppression; lifetime; cell membrane permeability; HeLa-cell water

### Introduction

Selective monitoring of the  $^1\text{H}$  magnetic resonance (MR) signal from intracellular water in cultured mammalian cell systems would allow characterization of biophysical properties of intracellular water that are important for quantitative interpretation of MR signals from tissue *in vivo*. Several methods have been proposed to discriminate intra- and extracellular water MR signals in biological systems such as cell suspensions, perfused cells, and intact tissues (1). These methods are based upon differences in the MR properties of intra- and extracellular water, including resonance frequencies (2–6), longitudinal or transverse relaxation times (7–9), and diffusion coefficients (10–12).

The method presented here, which employs a microbead-adherent (stationary) cell system, takes advantage of the high-velocity, turbulent flow of extracellular perfusate. In the presence of a slice-selective, spin-echo pulse sequence, the flow results in very rapid *apparent*

longitudinal and transverse relaxation (13–16) of extracellular water in the slice of interest. The flow-driven influx (washin) of equilibrium-state spins quickly returns extracellular water in the slice to full (equilibrium) longitudinal polarization. Rapid, turbulent flow in the presence of slice-selective RF pulses and strong concomitant gradient pulses results in efficient destruction of transverse phase coherence. Additionally, flow-driven efflux (washout) of spins from the slice also serves to diminish transverse magnetization.

Three benefits accrue from the situation in which the flow-dominated apparent transverse and longitudinal relaxation of extracellular water is very rapid; put more precisely, when the apparent transverse and longitudinal relaxation times of extracellular water are much shorter than the exchange lifetime of extracellular water. First, the signal contribution from extracellular water is completely suppressed due to flow (very rapid apparent transverse relaxation). Thus, the acquired MR signal arises only from intracellular water. Second, solutions to the Bloch-McConnell equations (17,18) for two-site (intracellular/extracellular) exchange are greatly simplified. Of particular interest herein, longitudinal relaxation of intracellular water is defined by an observed monoexponential magnetization recovery curve whose defining rate constant,  $(T_{1,obs})^{-1}$ , is the sum of two rate constants,

$$(T_{1,obs})^{-1} = (T_{1,in})^{-1} + (\tau_{in})^{-1}, \quad [1]$$

where  $T_{1,obs}$  is the observed exchange-modified longitudinal relaxation time for intracellular water,  $T_{1,in}$  is the *inherent* spin-lattice relaxation time constant for intracellular water – that which would be measured in the absence of the effects of exchange with extracellular water, and  $\tau_{in}$  is the intracellular water exchange lifetime. (Note, first order rate constants are expressed herein explicitly as the inverse of the relevant exponential time constant.) In essence, the exchange of water between the two compartments provides an additional relaxation pathway for intracellular water. Indeed, in the limit at which the exchange process completely overwhelms the inherent spin-lattice relaxation process, *i.e.*, when

$$(\tau_{in})^{-1} \gg (T_{1,in})^{-1}, \quad [2]$$

the observed relaxation time for intracellular water is identically the exchange lifetime,

$$(T_{1,obs})^{-1} = (\tau_{in})^{-1}. \quad [3]$$

In what follows, we show for a perfused, microbead-adherent HeLa cell system that: (i) the apparent relaxation of extracellular water is dominated by flow effects, (ii) the apparent relaxation is sufficiently rapid to completely suppress signal from extracellular water, (iii) the intracellular longitudinal relaxation is slow relative to exchange of water between the intracellular and extracellular compartments, being nearly described by Eq. [3], and, thus, (iv) this method, when combined with an inversion recovery pulse sequence, yields the intracellular water lifetime.

While the effects of flow in MR are well studied (14,16,19,20), to our knowledge, this is the first time this method has been used to separate intracellular and extracellular water signals, as well as measure intracellular water lifetime. This procedure should be applicable with any microbead-adherent cell type and is described herein as a “proof of principle” study applied to the robust HeLa cell line.

## Materials and Methods

Suppression of the extracellular water signal *via* the slice-selective spin echo experiment and the flow-dominance of apparent longitudinal and transverse relaxation were first verified by measuring the dependence of the MR signal amplitude on the perfusate flow rate (higher flow rates giving greater suppression of extracellular water signal) in microbead systems with and without HeLa cells present. The slice-selective inversion recovery spin echo experiment was then employed in the presence of HeLa cells and flowing perfusate to measure the exchange-modified longitudinal relaxation time of intracellular water ( $T_{1,obs}$ ). An independent cell relaxation measurement was made for pelleted cells without media to estimate the intracellular water longitudinal relaxation time in the absence of exchange ( $T_{1,in}$ ). The lifetime of intracellular water ( $\tau_{in}$ ) was then derived using Eq. 1.

### HeLa Cell Culture and Perfusion Procedures

**Cell culture and perfusion**—HeLa cells were grown as monolayers on polystyrene microcarrier beads (Nalge Nunc, Rochester, NY, USA) of 160 ~ 300 $\mu$ m diameter. Cells were cultured in a 95% O<sub>2</sub>/5% CO<sub>2</sub> atmosphere (37°C) for three days to reach confluence in Dulbecco's Modified Eagle's Medium (DMEM) supplemented with 10% (v/v) fetal calf serum, 2 mM L-glutamine, 100 units/ml penicillin and 100  $\mu$ g/ml streptomycin. Microbeads coated with cells were transferred to a 6.0-mm-ID glass tube. Pre-warmed media equilibrated with 95% O<sub>2</sub> and 5% CO<sub>2</sub> was pumped through the glass tube and a ball-float flow meter was used to monitor the volumetric perfusion rate. During the time it takes for perfusion media to travel from the face of the magnet to the sample tube it becomes completely (Boltzman) polarized. A fiber optic probe was inserted into the glass tube to monitor the temperature (37°C). For control experiments without cells, microcarrier beads only were placed in the media for three days and transferred to the MR sample tube.

**Cell Pellets**—For experiments performed on cell pellets, cells were cultured in a 162-cm<sup>2</sup> flask for three days to reach confluence, then washed with PBSA solution (the calcium- and magnesium-free Dulbecco's Phosphate Buffered Saline solution A) and trypsin for 5 minutes to release cells off the flask. Cell pellets were prepared by centrifugation at 400 g in a 50-ml centrifuge tube for 3 min. Cells were then transferred to a 4-mm-ID glass tube and centrifuged at 3000 g for 2 min. Cell pellets prepared by this procedure have less than 5% extracellular water (21). MR measurements were finished within 30 min of centrifugation at ~ 17°C.

**Other Procedures**—Light microscopic images of cells on beads were acquired with a Nikon Diaphot 300 microscope.

### MR experiments

**General**—All <sup>1</sup>H MR experiments were performed in a 4.7-T, 40-cm horizontal Oxford Instruments (Abingdon, Oxfordshire, UK) magnet equipped with a 10-cm inner diameter Magnex Scientific (Kidlington, Oxfordshire, UK) gradient set, a Techron (Elkhart, IN, USA) model 8300 gradient power supply, and a Varian (Palo Alto, CA, USA) *UNITYINOVA* console. Bayesian analysis was used to estimate signal amplitude of the acquired time-domain data and relaxation times from the inversion recovery data (22–24).

**Velocity-sensitive spin echo <sup>1</sup>H MR experiments**—An 8-mm-wide piece of copper foil was wrapped around the perfusion sample tube to serve as a <sup>1</sup>H transmit/receive solenoid coil. A 100- $\mu$ m-thick slice oriented orthogonal to the flow direction was defined by frequency selective  $\pi$  and  $\pi/2$  pulses (4 ms) in the presence of slice selection gradients (23 G/cm) applied parallel to the flow direction; TE = 25 ms, TR = 10 s. Only the second half of the echo was acquired. The acquisition time was 120 ms. Signals from 10 different slices spaced 300  $\mu$ m

apart were acquired in an order opposite to the flow direction. To improve signal-to-noise ratio (SNR), four signal averages were taken by cycling four times through the 10 slices. The volumetric perfusion rate ranged from 0 to 125 ml/min depending upon experimental purposes. Two sets of data were acquired respectively from the perfused cell-bearing microbeads and from the control sample -- microbeads without cells.

**Inversion recovery  $^1\text{H}$  MR experiments**—A slice-selective inversion pulse was inserted before the slice-selective, spin-echo sequence to measure the exchange-modified longitudinal relaxation time of intracellular water. The inversion time TI was incremented from 3.5 ms to 3.8 s. The time delay before each inversion pulse was longer than five times the measured relaxation time. Variable concentrations (0 mM, ~5 mM, ~15 mM) of Gadodiamide (Omniscan, Amersham Health) were added to the media to produce different inherent spin-lattice relaxation times of the extracellular media, *i.e.*, that which would be measured in the absence of flow. Samples of media with Gadodiamide were collected after the perfusion experiment and the inherent spin-lattice relaxation time was measured from each sample with an inversion recovery pulse sequence.

The HeLa cell intracellular water longitudinal relaxation time in the absence of exchange was estimated from cell pellets *via* a slice-selective inversion recovery spin echo pulse sequence with a laboratory-constructed, 6-mm-ID solenoid coil at TE = 25 ms and slice-thickness = 100  $\mu\text{m}$ . Inversion times ranged from 3.5 ms to 16 s. A 10-s time delay prior to each inversion pulse was used to ensure complete recovery of magnetization. Four signal averages were obtained.

## Results

Based on light microscopy (Fig. 1), HeLa cells have the shape of a half-sphere on the surface of microbeads, and the average diameter of these half spheres is 20  $\mu\text{m}$ . In the perfusion system, the volume ratio of intracellular to extracellular water was approximately 5%, estimated from cell diameter, cell number, bead weight, bead density and bead powder density; the latter two parameters provided by the manufacturer. In experiments with perfusion media flowing through a collection of *cell-free* packed microbeads, the water signal amplitude from the perfusion media (circles, Fig. 2) diminished into the noise as the flow rate of the perfusion media increased. However, in the equivalent experiments employing microbeads with attached cells, the water signal amplitude (triangles, Fig. 2) reached a plateau with SNR 40, well above the noise floor. Figure 3 shows representative  $^1\text{H}$  MR spectra from cell-free packed microbeads (A and C) and microbeads with attached cells (B and D). In the plateau region of Fig. 2 (triangles), the signal acquired from perfused cells shows a very slight decrease as flow rate increases. This may reflect a population of water molecules closely associated with the external surface of the cell membrane exiting the slice at the progressively higher flow velocities.

The longitudinal magnetization recovery time constant observed with the microbead-adherent cells in the presence of high velocity perfusion ( $T_{1,\text{obs}}$ ) was  $109 \pm 12$  ms ( $n = 3$ ). The value of  $T_{1,\text{obs}}$  did not change appreciably as the inherent spin-lattice relaxation time of the media was reduced from 2.5 s to 10 ms with the addition of Gadodiamide (Fig. 4). (Note, the assessment of signal amplitude at ~ 15 mM Gadodiamide concentration – ~ 10 ms relaxation time – was difficult because the linewidth of the observed water resonance broadened from 20 Hz to 300 Hz, presumably due to inhomogeneous bulk susceptibility effects.) The inherent intracellular water spin-lattice relaxation time ( $T_{1,\text{in}}$ ) was estimated from packed cells (pellets) as  $1.19 \pm 0.06$  s ( $n = 3$ ) at ~ 17°C. (At 37°C this value will increase by ~ 10% (25)). The intracellular water lifetime at 37°C ( $\tau_{\text{in}}$ ) was calculated as  $119 \pm 14$  ms using Eq. [1].

## Discussion

As noted earlier, the two-site, exchange-modified Bloch equations take on a simplified form when the apparent transverse and longitudinal relaxation times of extracellular water are much shorter than the exchange lifetime of extracellular water. At high perfusion velocities, the apparent relaxation times of extracellular water should be flow dominated and very short.

The inherent spin-lattice relaxation time of the perfusion media in the absence of relaxation agent was measured to be 2.5 s (data not shown). Although the process is unlikely to be purely monoexponential, a “pseudo time constant” describing reestablishment of longitudinal magnetization due to flow, specifically slice-specific washin of media, can be estimated as  $0.63 V_0/v$ , where  $V_0$  is the media volume of the selected slice and  $v$  is the volumetric flow rate (20). In our perfusion system,  $V_0$  is calculated from the slice thickness, glass tube diameter, and the fractional volume occupied by the microbeads in the glass sample tube. When  $v$  is 125 ml/min, the derived time constant is  $\sim 0.5$  ms. Comparing the two time constants, 0.5 ms vs. 2.5 s, it is clear that flow-driven reestablishment of longitudinal magnetization is far more efficient than the inherent spin-lattice relaxation of the perfusion media. Thus, flow dominates the apparent longitudinal relaxation of extracellular water.

The inherent transverse relaxation time of the media is 0.7 s (data not shown). The pseudo time constant describing loss of transverse magnetization due to flow is expected to be even shorter than that describing reestablishment of longitudinal magnetization due to flow. This is because, in addition to the slice-specific washout of media, turbulent flow (variable velocities) in the presence of the strong field gradients required for slice-selection severely drives loss of transverse magnetization phase coherence. A pseudo time constant governing loss of transverse magnetization due to flow can be independently estimated from the decrease in signal amplitude acquired from the perfusion media flowing through cell-free packed microbeads. At flow rates higher than 40 ml/min, a signal attenuation of at least 99% was observed with TE = 25 ms (circles, Fig. 2). This implies a time constant describing loss of transverse magnetization due to flow of significantly less than 4.6 ms at 125 ml/min. Again, flow-driven loss of transverse magnetization is far more efficient than the inherent transverse relaxation of the perfusion media. Thus, flow dominates the apparent transverse relaxation of extracellular water.

The equilibrium condition requires an equal rate of water exchange between the two compartments and, thus, that the lifetimes of intracellular and extracellular compartments ( $\tau_{in}$  and  $\tau_{ex}$ ) are proportional to the aqueous population fractions of the two compartments ( $f_{in}$  and  $f_{ex}$ ),

$$f_{in}(\tau_{in})^{-1} = f_{ex}(\tau_{ex})^{-1}; f_{in}/f_{ex} = \tau_{in}/\tau_{ex} \quad [4]$$

Given  $f_{in} / f_{ex} \sim 5/100$  and, as will be discussed below,  $\tau_{in} \sim 100$  ms,  $\tau_{ex}$  is then on the order of 2 s for the microbead-adherent HeLa cell system under study. Thus, the conditions required to simplify the Bloch equations hold. Specifically, the apparent transverse and longitudinal relaxation times of extracellular water ( $\sim 1$  ms) are much shorter than the exchange lifetime of extracellular water (2 s).

The ratio of MR signal amplitudes when microbead-adherent cells are perfused at flow rates 125 and zero ml/min is  $\sim 9\%$  in Fig. 2 (triangles). Correcting for relaxation and diffusion effects in the two compartments gives an MR determined water volume ratio of  $\sim 8\%$ . This value is consistent with the roughly estimated intracellular water volume ratio of  $\sim 5\%$ . However, while perfusion media signal suppression was complete with packed microbeads *in the absence of*

*adhering HeLa cells*, extracellular media “trapped” in the presence of adhering cells could contribute to the residual signal amplitude shown in Fig. 2 (triangles). However, if this were the case, the observed longitudinal relaxation time would be expected to decrease markedly with the addition of relaxation agent to the extracellular media. Such a decrease was not observed. Indeed, despite a reduction in the inherent spin-lattice relaxation time of the perfusion media from 2.5 s to 14 ms, the longitudinal relaxation time of the residual signal did not change appreciably (Fig. 4). This provides further evidence that longitudinal relaxation of extracellular water is fully flow dominated and gives no support for the putative presence of a semi-static pool of extracellular water that would contribute to the signal at high perfusion flow rate.

Measurement of the intracellular longitudinal relaxation time of packed HeLa cells gives an estimate for  $T_{1,in}$  of 1.2 s, which is consistent with the results reported by Wheatley *et. al.* (25) but is considerably longer than the value of 0.7 s reported by Beall *et. al.* (26). While packed cells are probably in a hypoxic/anoxic state, it is unlikely that the intracellular  $T_1$  is highly sensitive to oxygenation status. Numerous tissues *in vivo*, for which cell densities are high and capillary beds provide efficient oxygen delivery, have  $T_1$  values  $\sim 1$  s and show only modest  $T_1$  changes in death. Thus, cell pellets offer a reasonable means to estimate  $T_{1,in}$ . For the derivation of  $\tau_{in}$ , it is not crucial that the estimate of  $T_{1,in}$  be highly accurate given that  $T_{1,in}$  is clearly much greater ( $\sim$  ten fold) than the measured  $T_{1,obs}$  (1.2 s vs. 0.11 s). Specifically, given this differential, the accurate determination of intracellular water lifetime,  $\tau_{in}$ , *via* Eq [1] depends primarily on the measurement of  $T_{1,obs}$ . Indeed, the derived  $\tau_{in}$ , 0.12 s, is essentially equivalent to  $T_{1,obs}$ , 0.11 s; the system is close to the regime, Eq. [2], where the limiting case of Eq. [3] holds.

If Fick’s law holds true for water exchanging through the cell membrane, the intracellular water lifetime,  $\tau_{in}$ , is related to the cell membrane permeability,  $P$ , through the following relation (7,27):

$$P = V_{in} / (A \tau_{in}), \quad [5]$$

where  $P$  is the membrane permeability coefficient (cm/s),  $V_{in}$  is the total cell volume, and  $A$  is the cell surface area. The HeLa cell volume is  $2.6 \times 10^3 \mu\text{m}^3$  as estimated from the cell diameter measured under the light microscope. The surface area of the half-spherical microbead-attached cell, not including the area in contact with the microbead, is  $7.2 \times 10^2 \mu\text{m}^2$ . The cell membrane diffusional permeability calculated *via* Eq. [5] is  $3.6 \times 10^{-3}$  cm/s. The above value for the cell surface area is likely an underestimate because the cell surface is not smooth. Nevertheless, the estimated permeability is within the range reported by others for mammalian cells using very different methodologies (9,28). This agreement supports the validity of the MR-based method described herein.

## Conclusion

A method has been developed to select the intracellular water MR signal from perfused, microbead-adherent mammalian cells using a flow-related extracellular water MR signal suppression mechanism. When a thin MR excitation slice is defined, the high rate of perfusate flow acts as a very efficient apparent longitudinal and transverse relaxation mechanism for extracellular water (perfusion media) in the slice. Using a slice-selective spin echo pulse sequence, MR signal from the extracellular compartment is strongly suppressed, providing for selection of the intracellular water signal. The striking difference in the intra- and extracellular compartmental relaxation time constants under these conditions provides the means to derive the intracellular water lifetime,  $\tau_{in}$ , from the exchange-modified longitudinal relaxation of intracellular water. In HeLa cells,  $\tau_{in}$  was estimated to be 0.12 s. This defines a time scale for



measuring physical properties inherent to intracellular water in cultured HeLa cells. The methodology developed here should be applicable to a wide range of other microbead-adherent cultured mammalian cells. It provides a valuable tool to probe the properties of intracellular water in cultured mammalian cells. Such measurements can provide biophysical parameters critical to our understanding of the MR signal arising from mammalian tissue *in vivo*.

## Acknowledgments

The authors thank Z. M. Bhujwalla and E. Ackerstaff for their help in building the perfusion system, J. Prior for her support in cell culturing, X. Yu for her help with the light microscopic imaging, and G. L. Bretthorst for assistance in applying Bayesian signal analysis methods (see <http://bayesiananalysis.wustl.edu/>). This research was supported by NIH grants NS035912, EB002083, CA94056 and CA083060 from the Small Animal Imaging Research Program. J. J. Neil is also supported by the Green Chair in Pediatrics and Neurology.

## Abbreviations

$A$	the cell surface area
$f_{\text{ex}}$	aqueous population fraction of the extracellular compartment
$f_{\text{in}}$	aqueous population fractions of the intracellular compartment
$P$	the cell membrane permeability
$T_{1,\text{obs}}$	the observed exchange-modified longitudinal relaxation time for intracellular water
$T_{1,\text{in}}$	the <i>inherent</i> spin-lattice relaxation time constant for intracellular water
$V_0$	the media volume of the selected slice
$V_{\text{in}}$	the total cell volume
$\tau_{\text{ex}}$	the extracellular water exchange lifetime
$\tau_{\text{in}}$	the intracellular water exchange lifetime
$v$	the volumetric flow rate of perfusion media

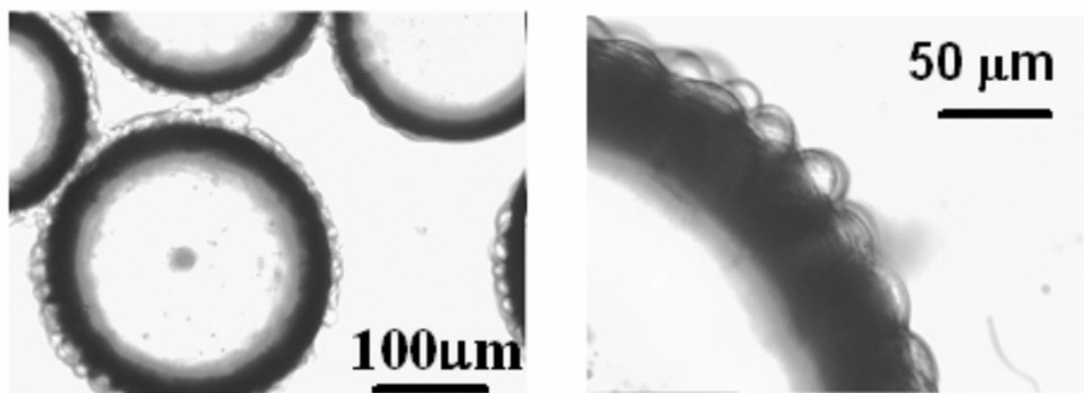
## References

1. Hills BP, Belton PS. NMR studies of membrane transport. Annual reports on NMR spectroscopy 1989;21:99–161.
2. Fritz OG Jr, Swift TJ. State of water in polarized and depolarized frog nerves. Proton magnetic resonance study. Biochem J 1967;7:675–687.

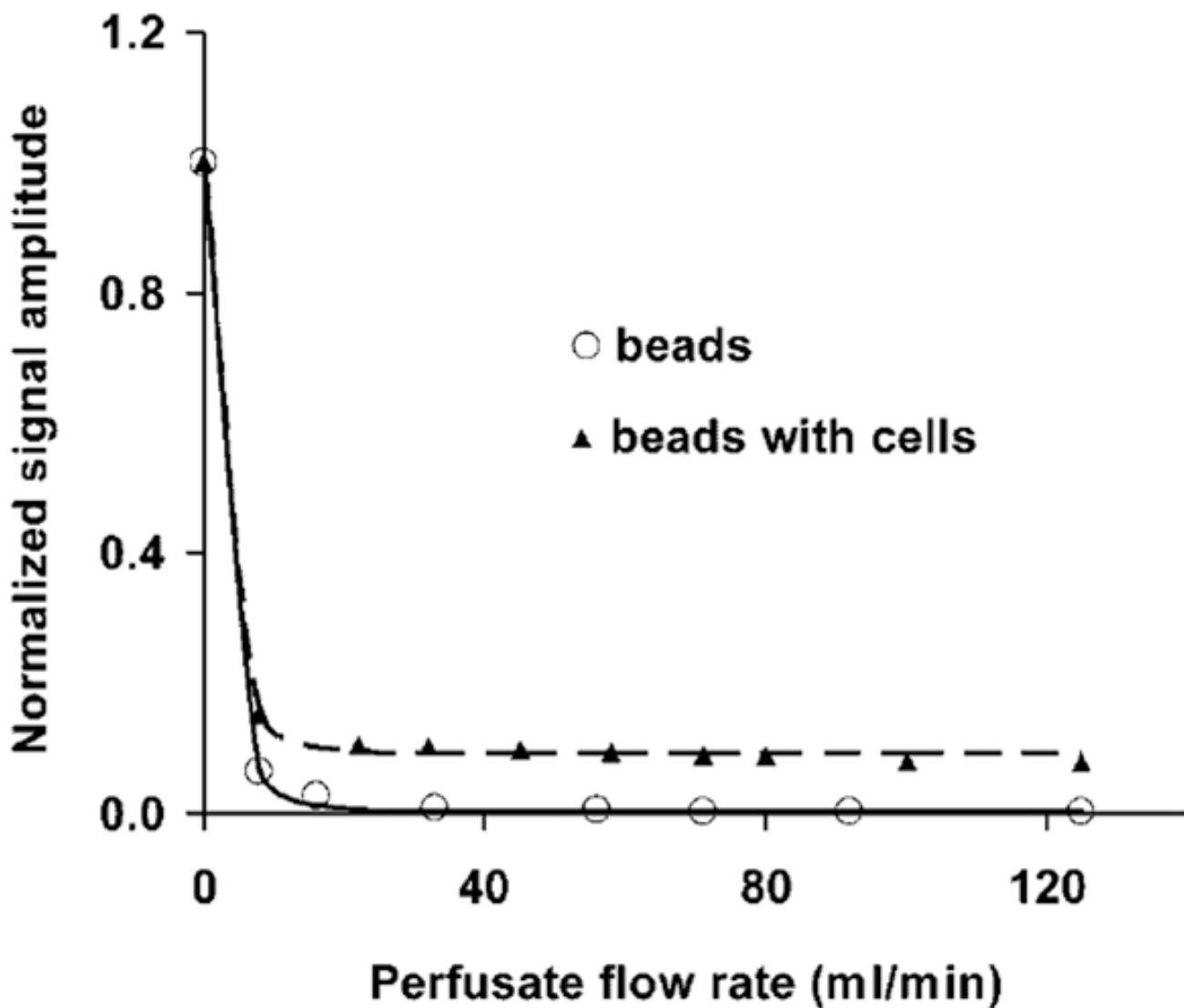
3. Naritomi H, Kanashiro M, Sasaki M, Kuribayashi Y, Sawada T. In vivo measurements of intra- and extracellular Na<sup>+</sup> and water in the brain and muscle by nuclear magnetic resonance spectroscopy with shift reagent. *Biophys J* 1987;52:611–616. [PubMed: 3676441]
4. Zhong K, Li X, Shachar-Hill Y, Picart F, Wishnia A, Springer CS Jr. Magnetic susceptibility shift selected imaging (MESSI) and localized <sup>1</sup>H<sub>2</sub>O spectroscopy in living plant tissues. *NMR Biomed* 2000;13:392–397. [PubMed: 11114062]
5. Galons JP, Lope-Piedrafita S, Divijak JL, Corum C, Gillies RJ, Trouard TP. Uncovering of intracellular water in cultured cells. *Magn Reson Med* 2005;54:79–86. [PubMed: 15968680]
6. Humpfer E, Spraul M, Nicholls AW, Nicholson JK, Lindon JC. Direct observation of resolved intracellular and extracellular water signals in intact human red blood cells using <sup>1</sup>H MAS NMR spectroscopy. *Magn Reson Med* 1997;38:334–336. [PubMed: 9256115]
7. Conlon T, Outhred R. Water diffusion permeability of erythrocytes using an NMR technique. *Biochim Biophys Acta* 1972;288:354–361. [PubMed: 5082996]
8. Herbst MD, Goldstein JH. A review of water diffusion measurement by NMR in human red blood cells. *Am J Physiol* 1989;256:C1097–C1104. [PubMed: 2719098]
9. Quirk JD, Bretthorst GL, Duong TQ, Snyder AZ, Springer CS Jr, Ackerman JJ, Neil JJ. Equilibrium water exchange between the intra- and extracellular spaces of mammalian brain. *Magn Reson Med* 2003;50:493–499. [PubMed: 12939756]
10. Van Zijl PC, Moonen CT, Faustino P, Pekar J, Kaplan O, Cohen JS. Complete separation of intracellular and extracellular information in NMR spectra of perfused cells by diffusion-weighted spectroscopy. *Proc Natl Acad Sci U S A* 1991;88:3228–3232. [PubMed: 2014244]
11. Pilatus U, Shim H, Artemov D, Davis D, van Zijl PC, Glickson JD. Intracellular volume and apparent diffusion constants of perfused cancer cell cultures, as measured by NMR. *Magn Reson Med* 1997;37:825–832. [PubMed: 9178232]
12. Pfeuffer J, Flogel U, Leibfritz D. Monitoring of cell volume and water exchange time in perfused cells by diffusion-weighted <sup>1</sup>H NMR spectroscopy. *NMR Biomed* 1998;11:11–18. [PubMed: 9608584]
13. Zhernovoi, AI.; Latyshev, GD. NMR in a Flowing Liquid. Plenum Press; New York: 1965. Introduction; p. 1-7.
14. Jones DW, Child TF. NMR in Flowing System. *Advances in Magnetic Resonance* 1976;8:123–148.
15. Hemminga MA, De Jager PA, Sonneveld A. The study of flow by pulsed magnetic resonance. I. Measurement of flow rates in the presence of a stationary phase using a difference method. *J Magn Reson* 1977;27:359–370.
16. Dorn, HC.; Flow, NMR. *Encyclopedia of Nuclear Magnetic Resonance*. Grant, DM.; Harris, RK., editors. John Wiley & Sons; New York: 1996. p. 2026-2037.
17. Forsen S, Hoffman RA. Study of moderately rapid chemical exchange reactions by means of nuclear magnetic double resonance. *J Chem Phys* 1963;39:2892–2901.
18. McConnell HM. Reaction rates by nuclear magnetic resonance. *J Chem Phys* 1958;28:430–431.
19. Zhernovoi, AI.; Latyshev, GD. NMR in a Flowing Liquid. New York: Plenum Press; 1965.
20. Lee JH, Li X, Sammi MK, Springer CS Jr. Using flow relaxography to elucidate flow relaxivity. *Journal of Magnetic Resonance* 1999;136:102–113. [PubMed: 9887295]
21. Wheatley DN, Rimmington JE, Foster MA. Effects of osmotic manipulation of intracellular hydration of HeLa S-3 cells on their proton NMR relaxation times. *Magn Reson Imaging* 1990;8:285–293. [PubMed: 2366640]
22. Bretthorst GL, Hutton WC, Garbow JR, Ackerman JJH. Exponential parameter estimation (in NMR) using Bayesian probability theory. *Concepts in Magnetic Resonance, Part A* 2005;27A:55–63.
23. Bretthorst GL, Hutton WC, Garbow JR, Ackerman JJH. Exponential model selection (in NMR) using Bayesian probability theory. *Concepts in Magnetic Resonance, Part A* 2005;27A:64–72.
24. Bretthorst GL. How accurately can parameters from exponential models be estimated? A Bayesian view. *Concepts in Magnetic Resonance, Part A* 2005;27A:73–83.
25. Wheatley DN, Redfern A, Johnson RP. Heat-induced disturbances of intracellular movement and the consistency of the aqueous cytoplasm in HeLa S-3 cells: a laser-Doppler and proton NMR study. *Physiol Chem Phys Med NMR* 1991;23:199–216. [PubMed: 1812500]



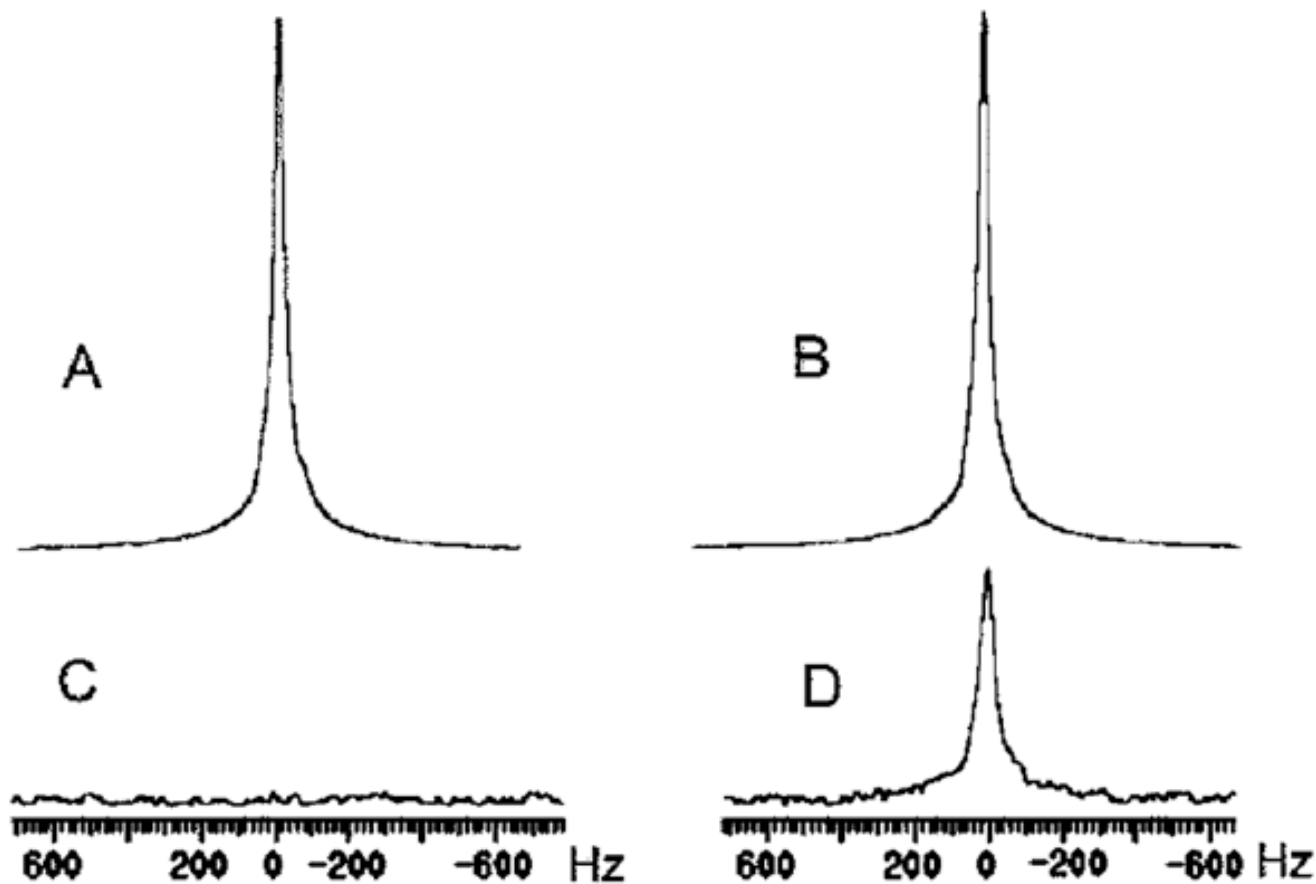
26. Beall PT, Hazlewood CF, Rao PN. Nuclear magnetic resonance patterns of intracellular water as a function of HeLa cell cycle. *Science* 1976;192:904–907. [PubMed: 1273575]
27. Chen ST, Springer CS Jr. Ionophore-catalyzed cation transport between phospholipid inverted micelles manifest in DNMR. *Biophys Chem* 1981;14:375–388. [PubMed: 17000180]
28. House CR. Water transport in cells and tissues. *Monogr Physiol Soc* 1974;24:156.



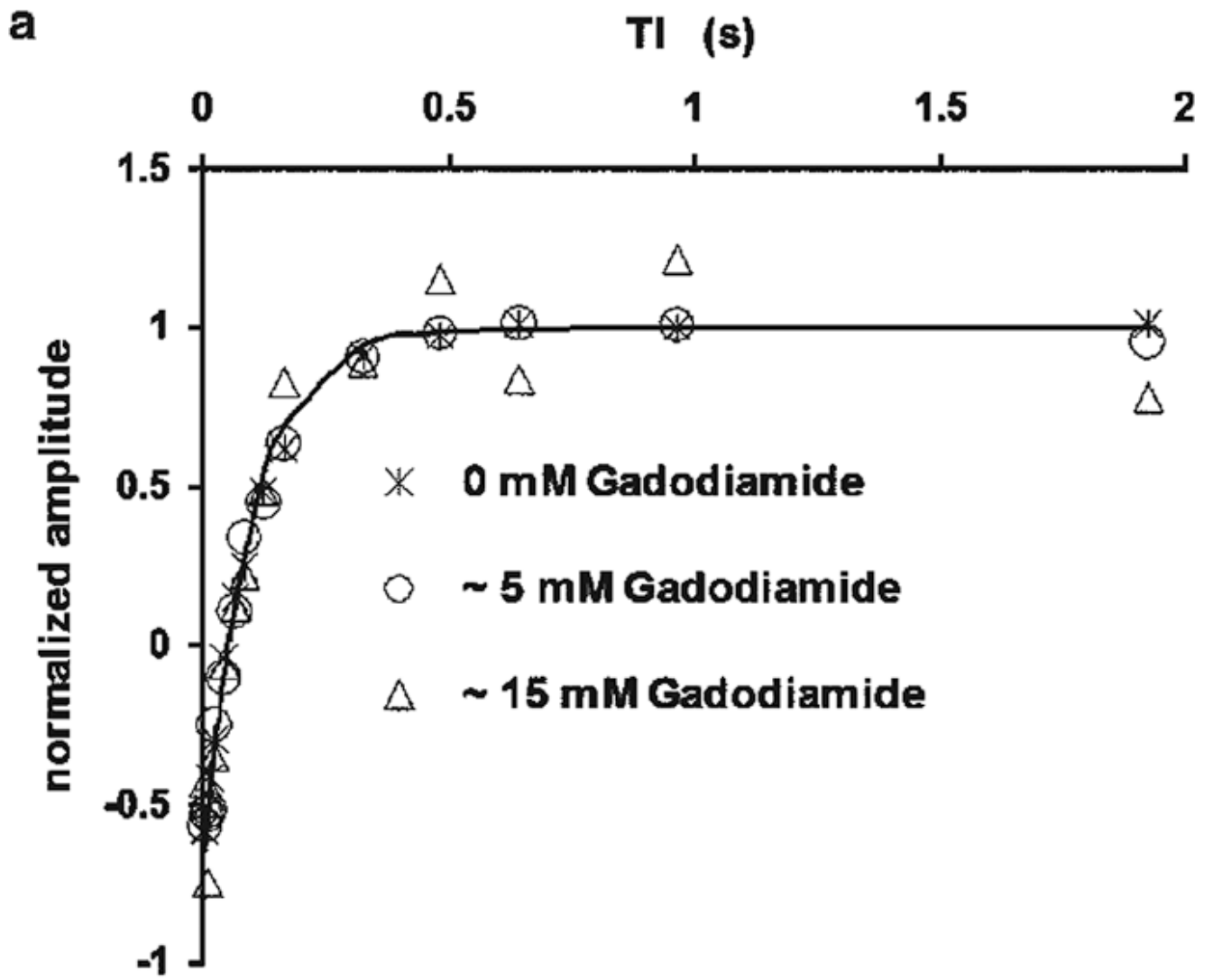
**Figure 1.**  
Light microscopic image of HeLa cells on microbeads. The dark rim is the edge of the microbeads and the bulbs on the surface of the microbeads are cells.



**Figure 2.** Representative example of signal amplitude (average from ten slices) vs. perfusion rate (circles, microbeads only; triangles, microbeads with attached HeLa cells). At flow rates higher than 40 ml/min, circles are equivalent to the noise level.



**Figure 3.** Panels A and C:  $^1\text{H}$  spectra acquired from the perfusion media flowing through cell-free packed microbeads (A: 0 ml/min; C: 125 ml/min); panels B and D:  $^1\text{H}$  spectra acquired from perfused microbeads with attached cells (B: 0 ml/min; D: 125 ml/min); panels C and D have 10x vertical scale expansion. A 10-Hz line broadening exponential apodization function was applied before Fourier transformation.



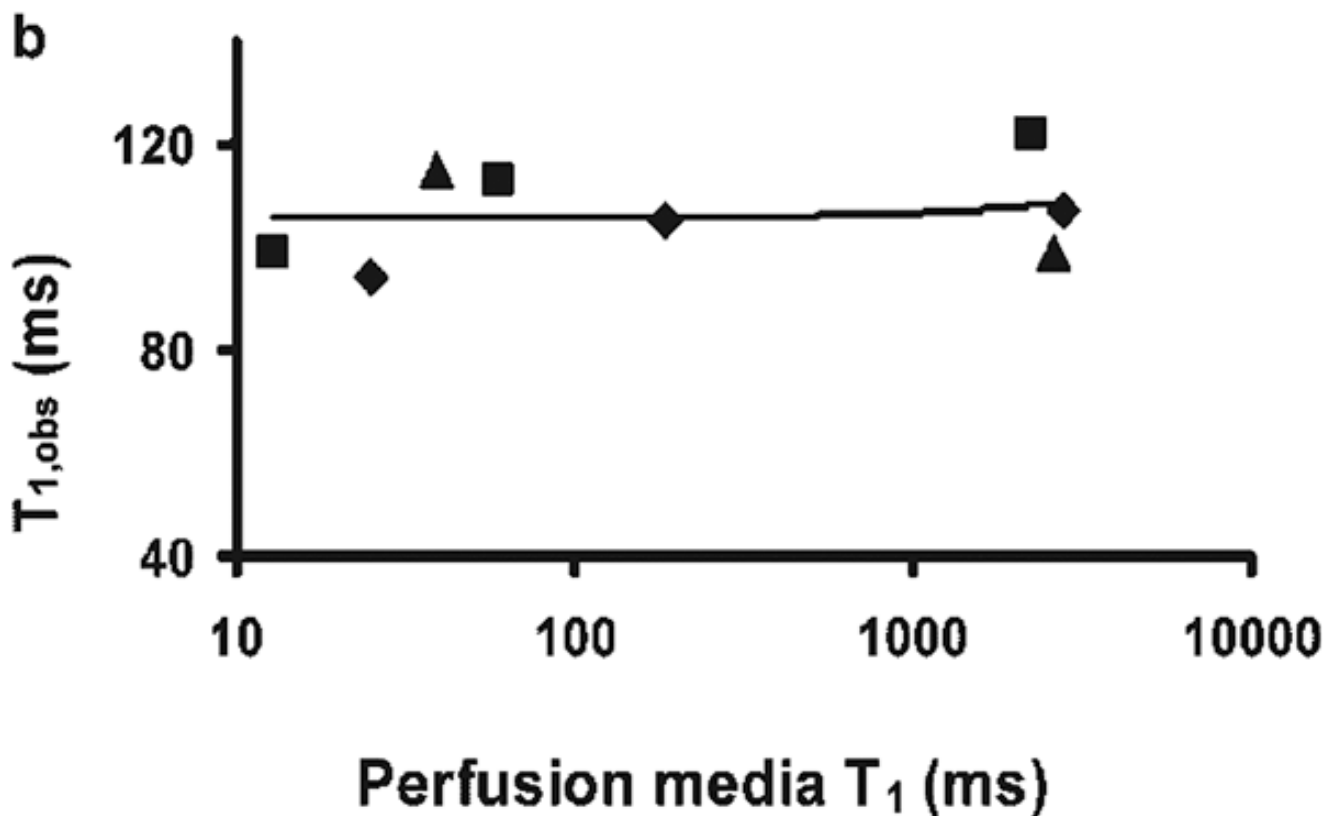


**Figure 4.**

**Figure 4a.** Normalized inversion recovery curves from a typical batch of perfused HeLa cells with various Gadodiamide concentrations (crosses, 0 mM; circles, ~ 5 mM; triangles, ~ 15 mM) in the perfusing media. The line is the modeled curve assuming monoexponential magnetization recovery for the data set of 0 mM Gadodiamide. The modeled curves of the other two sets of data are overlapping with this line. Data acquired at inversion times longer than 2 s are not shown. As the concentration of gadodiamide increases, the linewidth of the observed water resonance is broadened from 20 Hz to 300 Hz, presumably due to inhomogeneous bulk susceptibility effects. The assessment of water <sup>1</sup>H resonance amplitude at greater relaxation agent concentrations (shorter relaxation times) is increasingly uncertain.

**Figure 4b.** Exchange-modified longitudinal relaxation time measured from HeLa perfused cells on microbeads,  $T_{1,obs}$ , vs. the inherent spin-lattice relaxation time of perfusion media at different concentrations of Gadodiamide. Note that the x-axis scale is logarithmic. Different symbols represent different batches of cells. A linear regression curve is plotted through the data and its slope is 0.001. Because the x-axis is in logarithmic scale, the fitted linear curve does not appear to be a straight line.